RSC Advances

ROYAL SOCIETY OF CHEMISTRY

www.rsc.org/advances

Effects of functional groups of graphene oxide on the electrochemical performance in lithium-ion batteries

Zhengwei Xie[a,b], , Zuolong Yu[a], Weifeng Fan[a],Gongchang Peng[a], Meizhen Qu[*a]

[a] *Chengdu Institute of Organic Chemistry, Chinese Academy of Sciences, Chengdu 610041, PR China.*

[b] *Graduate University of Chinese Academy of Sciences, Beijing 100039, PR China.*

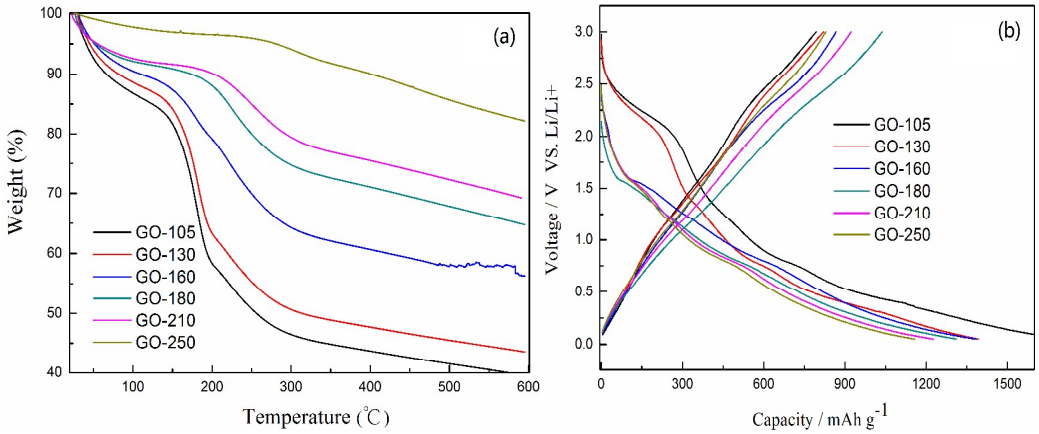

Fig. a displays the TGA plots, which show weight loss as a function of temperature for different GO. When the temperature is up to 180℃, the electrode presents the highest reversible capacity, as shown in Fig. b. However, further increasing the temperature, the capacity of GO electrodes begin to decline. Demonstrating not all of these functional groups can play a positive role in electrochemical performance.

* Corresponding author. *Fax: +86 28 85215069; Tel.: +86 28 85228839; E-mail: mzhqu@cioc.ac.cn, xiezhengwei116@hotmail.com*

Effects of functional groups of graphene oxide on the electrochemical performance in lithium-ion batteries

Zhengwei Xie[a,b], , Zuolong Yu[a], Weifeng Fan[a],Gongchang Peng[a], Meizhen Qu[*a]

[a] *Chengdu Institute of Organic Chemistry, Chinese Academy of Sciences, Chengdu 610041, PR China.*

[b] *Graduate University of Chinese Academy of Sciences, Beijing 100039, PR China.*

Abstract: Graphene oxide (GO) with different ratios of functional groups are prepared via low temperature directional thermal reduction and re-oxidization by nitric acid. The structure, elemental, oxygen-containing functional groups compositions and electrochemical behaviors of prepared GO are characterized by Fourier infrared spectrometer, X-ray diffraction, Thermogravimetric analysis, Raman spectrum, X-ray photoelectron spectroscopy, as well as charge/discharge curves and the electrochemical impedance spectra measurements. Compared with the graphite and graphene, the enhanced reversible capacity of GO is attributed to the oxygen-containing functional groups and contributed capacities are attributed dominantly to carbonyl and carboxyl. Besides, the labile oxygen functionality, such as epoxy, has the negative effect on electrochemical properties, which lowered the initial coulomb efficiency of graphene oxide anode materials. These findings may be beneficial to the material design of graphene-based anode materials with high energy density.

Keywords: graphene oxide; epoxy; carbonyl; carboxyl; specific capacity

[*] Corresponding author. *Fax: +86 28 85215069; Tel.: +86 28 85228839; E-mail: mzhqu@cioc.ac.cn, xiezhengwei116@hotmail.com*

1 Introduction

Graphite, which is the most common anode material for current commercial Li ion batteries (LIBs), cannot fulfill the requirement of high-energy applications, because of its limited specific capacity, with a theoretical value of 372 mAh g^{-1}.[1-3] Different types of anode materials with high specific capacities have been proposed for LIBs. Among these anode materials, carbonaceous materials have cause the attention due to their low price and plentiful sources. Especially the graphene,[4-9] with double storage capacity of common graphite in theory, has been suggested to be an attractive candidate for potential applications in electrochemical energy storage. However, a higher costs, irreversible aggregation and the hazardous or toxic reducing agents ($NaBH_4$, hydrazine and formaldehyde) still seriously hinder its large-scale application.

As the precursor of graphene, graphene oxide (GO) has been widely used in supercapacitor,[10-12] fuel cells[13] and Li-ion batteries.[14-16] GO possess a higher capacity, outstanding cycling performance and can easily form self-assembly membrane instead of polymer binder because of the numerous functional groups, such as hydroxyl, epoxy, carbonyl, carboxyl and C=C double bond. However, not all of these functional groups can play a positive role in electrochemical performance, some of them are negative effects, such as higher irreversible Li ion consumption.

So far, there have been no final conclusion about the influences of different functional groups of GO to the electrochemical performance in LIBs. It has been reported that the carbonyl on the surfaces of carbon nanotubes can store lithium ion,[17] and the

materials with >C=O bond (carbonyl and carboxyl) used in Li-ion battery as cathode materials have also been proposed.[18,19] However, some different opinions were also appeared. Kuo et al.[20] thought that the additional capacity is predominantly attributed to phenol, but the carboxyl, lactone and carbonyl result in irreversible lithiation/de-lithiation processes. But Wang et al.[21] thought that the epoxide of GO can have a high capacity of 360.4 mA h g^{-1} at 50 mA g^{-1} as cathode material. Therefore, it is a meaningful thing to explore the roles of different functional groups of GO to play on the electrochemical performance for LIBs.

Thus, in this work, GO with different ratios of functional groups were prepared via low temperature directional thermal reduction technology in N_2 atmosphere. At the same time, the nondestructive covalent carboxyl-rich graphene oxide was prepared for first time by means of adjusting the ultrasonic time, ultrasonic power and the amount of nitrate acid. The Reduced GO (RGO) with less oxygen containing functional groups was also prepared by hydrazine as mentioned in the literature[22] to verify the role of the C=C double bond.

The prepared GO with different ratios of functional groups were investigated and applied as GO based anode materials for LIBs. It is worth noting that the amount of functional groups in the GO is related to processing temperature. The enhanced reversible capacity of GO electrode was attributed to the oxygen-containing functional groups and the contributed capacities were attributed dominantly to carbonyl and carboxyl, which had been proved by us.

2 Experimental

2.1 Preparation GO and GO electrodes with different ratios of functional groups

All chemical reagents used to prepare GO were analytical grade (purchased from Kelong Chemical Reagent Crop. Chengdu, China) and used as received. GO was synthesized from high-purity natural flake graphite (about 200 meshes, Changsha Shenghua Research Institute, 99.999%) by a modified Hummers method.[23,24] And the colloidal dispersion of GO in deionized water was prepared with the aid of ultrasound treatment (20 kHz ultrasound probe) about 30 min to give a stable amber dispersion. Subsequently, the products were washed with deionized water to remove the extra sulfuric acid and dried in vacuum at 60℃. The finally obtained samples were GO powders. 0.14 g GO powders were added to 300.0 mL of deionized water under ultrasound (20 kHz ultrasound probe) treatment about 30 min to give a stable brown dispersion in a 500 mL beaker. 0.06 g Super-P (Conductive additive, 40 nm, 62 m^2 g^{-1}, TIMCAL Graphite & Carbon) was added to the brown dispersion under stirring and sonication for 30 min, then the beaker was placed in 80℃ water bath to remove the excess water, and at last, the uniform slurry was obtained. The obtained slurry was coated onto Cu foil and dried at 105℃ for 12 h in the vacuum drying oven to remove the adsorbed water of GO surface, then the foil was cut into disks (10 mm in diameter). The decomposition temperature of different functional groups are related to the temperature, therefore, the GO treated with different temperature (130℃, 160℃, 180℃, 210℃ and 250℃) in N_2 were prepared and investigated as anode materials for LIBs, and the prepared electrodes were nominated as GO-105, GO-130, GO-160,

GO-180, GO-210 and GO-250, respectively. At the same time, the RGO and the carboxyl-rich GO were prepared to demonstrate the roles of C=C bond (C=C) and carboxyl (O-C=O). The RGO was fabricated by hydrazine[15,16] and the carboxyl-rich GO was prepared by means of adjusting the ultrasonic time, ultrasonic power and the amount of nitrate acid. As is well known, both the thickness and density of working electrodes can obviously affect the electrochemical performance of the batteries. To have an accurate comparison, the same thickness and density of working electrodes were prepared for electrodes.

2.2 Materials characterization

Fourier transform infrared spectroscopy (FT-IR) was used to identify the functional groups of GO treated with different temperature (Bio-Rad FTS-60VM FT-IR spectrometer), and the samples were mixed with KBr and then finely ground to produce a pellet for the FT-IR experiment. X-ray diffraction (XRD) patterns were obtained from X' Pert MPD DY1219 using Cu/K_α radiation (λ=1.5406 Å). Thermogravimetric analysis (TGA) was carried out on a TG209F1 (NET-ZSCH, Germany), at a heating rate of 10℃ min^{-1} from 30 to 600℃ in nitrogen atmosphere. Raman spectra were carried out by a Jobin-Yvon LabRAM HR 800 UV spectrometer with a 633 nm line of a He-Ne laser as the exciting source. Using Al/K_α radiation ($h\nu$=1486.6 eV), X-ray photoelectron spectroscopy (XPS, PHI5600 Physical Electronics) was used to determine elemental compositions and assignments of carbon peaks.

2.3. Electrochemical measurements

The coin cells were assembled with lithium metal as the counter electrode and a Celgard 2400 was employed as separator in a glove box filled with Ar gas. The electrolyte was obtained from Capchem. Technology (Shenzhen) Co., Ltd., consists of a solution of 1.0 M $LiPF_6$ in ethylene carbonate, dimethyl carbonate, diethyl carbonate (EC/DMC/DEC, 1:1:1, in volume). Galvanostatic discharge/charge experiments were carried out on an automatic galvanostatic charge-discharge unit (Land CT 2001A, Wuhan, China) under different current densities from 3.0 to 0.01 V at 25℃. Electrochemical impedance spectroscopy (EIS) tests were conducted on PARSTAT 2273 Electrochemical System (Princeton Applied Research, USA). The EIS measurements were performed at the input signal amplitude of 5 mV (vs. open circuit potential) and the frequency ranging from 10^5 Hz to 10^{-2} Hz, and the measured data were fitted by Z-View software (Scribner Associates Inc.). All the measurements mentioned above are based on the total mass of the active materials (GO).

3 Results and Discussion

Fig. 1a shows the reversible charge/discharge curves of the GO electrodes treated with different temperature. The charge capacity of the GO-105 is 701 mAh g^{-1} at 0.5C (1C=372 mA g^{-1}), which is twice of graphite, and also higher than graphene (700 mAh g^{-1} for theoretical and 600 mAh g^{-1} for actual). However, the discharge capacity of it is over 1600 mAh g^{-1}, so the initial coulomb efficiency of prepared electrode is only 50%, hindering its large-scale application. Additionally, in the region of 2.5~2.2 V, the GO-105 electrode has a higher irreversible capacity owing to the remaining water crystal water and hydrogen bonding of water, as the water can occur

electrochemical decomposition reaction in this voltage range.[25] With the increase of temperature, the irreversible consumption gradually disappear, and when the temperature is up to 160℃, the irreversible consumption disappears completely at this area. At the same time, it is observed that the reversible charge capacity increases gradually with the increasing of the temperature, and the GO-180 electrode presents the highest reversible capacity. However, further increasing the temperature, the capacity of GO-210 and GO-250 electrodes begin to decline. Because most of the contributed capacities functional groups can cause thermal decomposition over a certain temperature.

The EIS tests were used to further verify the electrochemical performance of prepared electrodes. Fig. 1b shows the EIS of the GO electrodes treated with different temperature. These AC impedance spectra are fitted by Z-View software[19,25] and shown in the inset of Fig. 1b (insert) and Table 1. Here R_s is the resistance of the electrolyte, R_{ct} the charge transfer resistance at the particle/electrolyte interface, W the Warburg impedance, representing the Li-ion diffusion process, constant phase element (*CPE*) represents the double-layer capacitance and C is the insertion capacitance at the applied potential. From Table 1, the R_{ct} of GO treated with different temperature present a trend of decreases first and then increases, and the GO-180 presents the lowest charge transfer resistance. These findings were consistent with the results of the charge and discharge curves (Fig. 1a).

To probe the fundamental mechanism for the variation of GO treated with different temperature, FT-IR was carried out to monitor the variation of the functional groups

of the GO with the change in temperature (Fig. 2a). For GO-105, six main adsorption bands are identified, respectively center at 840, 1050, 1225, 1625, 1730 and 3400 cm^{-1}. The bands at 840 and 1225 cm^{-1} are assigned to epoxy and epoxide groups,[26] the >C-O valence vibrations is found at 1050 cm^{-1} and O-H of water deformations at 1400 and 3400 cm^{-1}.[27] The weak band at 1730 cm^{-1} shows some >C=O stretching vibrations of carbonyl or carboxyl, which indicates a small amount of carbonyl and carboxyl groups within the GO.[28] The intensities of the peaks at 1250 cm^{-1}, 1050 cm^{-1}, and 840 cm^{-1} for GO decrease with the increasing of the temperature, especially the bands intensities at 840 and 1050 cm^{-1} are almost disappeared when the temperature is up to 180℃, indicating the epoxy and epoxide groups are instability and easily decomposes. Additionally, the band intensity at 1625 cm^{-1} is disappeared and the band intensity at 1580 cm^{-1} appeared at 180℃, which indicates all the water (crystal water and the water connected with hydrogen bond) is removed at this temperature and the C=C conjugate has a certain recover. With the loss of the water and epoxy groups, the intensity of >C=O becomes strengthened obviously at 1730 cm^{-1}.

To further verify the conclusion of FT-IR, the XRD was used to characterize the structure of as prepared electrodes materials. Fig. 2b displays the XRD patterns of GO treated with different temperature. The diffraction peak of exfoliated GO at $2\theta=9.5°$ (001) features a basal spacing of 0.94 nm (calculated by the Scherrer formula), showing the complete oxidation of graphite to GO due to the introduction of oxygen-containing functional groups onto the graphite sheets.[29] With the temperature

increasing, there is a slight shift of the diffraction peak towards higher angle, from 9.5° shifts to 24°, approaching the diffraction peak of the graphite at 26.5 (002), and the d-spacing reduce to 0.365 nm, suggesting the oxygen containing functional groups in-plane of GO, such as hydroxyl and epoxy, have been removed partly.

TGA was used to further assess the change of structure and functional groups of the GO treated with different temperature. Fig. 2c displays the TGA plots, which show weight loss as a function of temperature for different GO (at a heating rate of 5℃ min^{-1} under a nitrogen atmosphere). The TGA curve of GO-105 exhibits three degradation steps. The first degradation commences at 30℃, which is attributable to the loss of adsorbed water from the surface of GO. The second step degradation commences at 120℃ due to the loss of hydroxyl, epoxy functional groups and the remaining water molecules.[30,31] The third step degradation starts from 200℃ involved the pyrolysis of the stabilized oxygen-containing groups. With the temperature increasing, significant differences occurred in the second and third steps degradation. When the temperature is up to 180℃, the first and second steps degradation are nearly disappeared, which suggest that the residual water and most of the labile oxygen functionalities (such as epoxy group) have been removed from the GO at 180℃. These findings are consistent with the results of the FT-IR tests and XRD patterns. When the temperature is up to 210℃, the third step degradation are commenced, which illustrate that the carboxyl begin to decompose and these conclusion are consistent with the results of the charge and discharge curves (Fig. 1a) and the FT-IR tests (Fig. 2a).

Structure integrity of graphitic materials was confirmed by Raman spectroscopy. As shown in Fig. 2d, GO-105 exhibits a strong D band at ~1350 cm^{-1} and a G band at ~1600 cm^{-1}, corresponding to sp^3 and sp^2 of carbon atoms, respectively. The Raman spectra of GO treated with different temperature are shown in Fig. 2d. It is worth noting that the D/G intensity ratio (I_D/I_G) presents a trend of decreases first and then increases (I_D/I_G=0.98, 0.97, 0.95, 0.99, and 1.01). Because the loss of adsorbed water and the labile functional groups can be removed under a low temperature. However, when the temperature is up to 210℃, new GO domains are created and which are smaller in size to the ones present in initial GO, but more numerous in number.[32]

Fig. 3 illustrates XPS C1s spectra of the GO treated with different temperature and their curves fitting. Listed in Table 2 are XPS data in detail, it can be observed that the variation of content of functional groups along with the temperature. The hydroxyl and epoxy groups are reduce gradually and even disappeared with the increasing temperature, do not conform to the trend of capacity change with the temperature (Fig. 1a). Thus, the conclusion that the hydroxyl and epoxy groups have no contribution to the capacity of GO electrode are deduced. Only the variation of content of carboxyl is consistent with the variation of specific capacity, as shown in Fig. 1a, testifying the carboxyl play an important role in specific capacity. However, the roles of functional groups C=C bond and carbonyl to play on the electrochemical performance have not been ensure in detail.

In order to explore the effect of C=C bond on the electrochemical property of GO for LIBs, the RGO was fabricated by hydrazine. As shown in Fig. 4a, only a small

amount of hydroxyl is observed and the C=C conjugated structure is almost recovered. The rate capability of RGO is better than GO as the C=C bond has a better conductive ability. However, the GO has a higher specific capacity than RGO because the GO has more oxygen containing functional groups, which can store more Li ions[16]. In conclusion, the C=C bond play an important role in rate performance, but has no contribution to the capacity of GO electrode for LIBs.

XPS was used to detection the variation of functional groups during the charge and discharge process. The GO-105 electrode before charge and discharge cycle, lithiated and de-lithiated state were characterized and shown in Fig 5. The GO-105 electrode without charge and discharge cycle test shows five peaks at 284.6, 286.6, 287.3, 288.2 and 289.1, which correspond to sp^2 hybridized carbon, hydroxyl (C-OH), epoxide (C-O-C), carbonyl (>C=O) and carboxyl (>O-C=O) functional groups, respectively (Fig. 5a). However, certain changes occur in the functional groups after it is subjected to a discharge-charge (lithiated and de-lithiated) process at 0.5C. A comparison of the peaks in Fig. 5a suggests the following facts. First, a new peak of nearly semi-ionic C-F group arises because of the side effects of the electrode and electrolyte[18]. Second, Comparison of the GO-105 electrode before electrochemical tests, the peaks intensity of carbonyl (>C=O) and carboxyl (>O-C=O) have reduced while the >C-OH strengthened obviously after lithiation process (Fig. 5b). However, there is an inverse process after delithiation process (Fig.5c), which prove the >C=O (carbonyl and carboxyl) and Li^+ can undergo reversible reaction, and these results agree well with the proposed hypothesis that the >C=O can improve the reversible charge capacity

and initial coulomb efficiency[17-19].

To prove the hypothesis that the >C=O can improve the reversible charge capacity, the carboxyl-rich GO was also prepared by means of adjusting the ultrasonic time, ultrasonic power and the amount of nitrate acid, nominated as GO-COOH. Compared with the initial GO, the GO-COOH (Fig. 5e) has a higher content of carbonyl and carboxyl, as shown in Table 3. Fig. 5f is the discharge/charge curves of GO and GO-COOH at 0.5 C, the GO-COOH electrode, with higher content of carbonyl and carboxyl, has a charge capacity of 1001 mAh g^{-1}, far higher than that of GO electrode (701 mAh g^{-1}).

Additionally, the prepared GO-COOH was adopted in (LGC) composite anode materials, which has been reported in our previous work[16]. The specific capacity of LTO/GO-COOH (LGCC) composite electrode has been increased by 10% than that of LGC electrode (shown in Fig. S1a). And the coulomb efficiency has been also improved greatly, from 70% to 82% (shown in Fig. S1b).

Acknowledgements

This work cannot be accomplished without the financial support from MOST of China (2011CB932604), the National Natural Science Foundation of China (grant no. 51302232) and the 973 Program (grant no.2013CB934700). Meanwhile our gratitude goes to Analytical and Testing Center of Chengdu Branch, Chinese Academy of Sciences.

References

1 O. M. Pan, H. B. Wang and Y. H. Jiang, J. Mater. Chem., 2007, 17, 329.

2 S. W. Lee, N. Yabuuchi, B. M. Gallant, S. Chen, B. S. Kim, P. T. Hammond and Y. Shao-Horn, Nat. Nanotechnol., 2010, 5, 531.

3 J. M. Tarascon and M. Armand, Nat., 2001, 414, 359.

4 D. Wang, R. Kou, D. Choi, Z. Yang, Z. Nie, J. Li, L. V. Saraf, D. Hu, J. Zhang, G. L. Graff, J. Liu, M. A. Pope and I. A. Aksay, ACS Nano, 2010, 4, 1587.

5 H. J. Kim, Z. H. Wen, K. H. Yu, O. Mao and J. H. Chen, J. Mater. Chem., 2012, 22, 15514.

6 C. C. Ma, X. H. Shao and D. P. Cao, J. Mater. Chem., 2012, 22, 8911.

7 E. Pollak, B. Geng, K. J. Jeon, I. T. Lucas, T. J. Richardson, F. Wang and R. Kostecki, Nano Lett., 2010, 10, 3386.

8 X. Zhao, C. M. Hayner, M. C. Kung and H. H. Kung, Adv. Energy Mater., 2011, 1, 1079.

9 P. Guo, H. H. Song, X. H. Chen, Electrochemistry Communications, 2009, 11, 1320.

10 J. Li, H. Q. Xie and Y. Li, J. Power Sources, 2013, 241, 388.

11 J. Li, H. Q. Xie and Y. Li, J. Nanosci. Nanotechnol., 2015, 15, 3280.

12 B. Xu, S. F. Yue, Z. Y. Sui, X. T. Zhang, S. S. Hou, G. P. Cao and Y. S. Yang, Energy Environ. Sci., 2011, 4, 2826.

13 L. S. Wang, A. N. Lai, C. X. Lin, Q. G. Zhang, A. M. Zhu, Q. L. Liu, J. Membr. Sci., 2015, 492, 58.

14 J. X. Zhang, H. Q. Cao, X. L. Tang, W. F. Fan, G. C. Peng and M. Z. Qu, J. Power Sources, 2013, 241, 619.

15 J. X. Zhang, Z. W. Xie, W. Li, S. Q. Dong and M. Z. Qu, Carbon, 2014, 74, 153.

16 Z. W. Xie, X. Li, W. Li, M. Z. Chen and M. Z. Qu, J. Power Sources, 2015, 273,

754.

17 L. Y. Wang, L. H. Zhuo, H. Y. Cheng, C. Zhang and F. Y. Zhao, J. Power Sources, 2015, 283, 289.

18 B. Z. Jang, C. G. Liu, D. Neff, Z. N. Yu, M. C. Wang, W. Xiong and A. Zhamu, Nano Lett., 2011, 11, 3785.

19 W. Ai, Z. Z. Du, Z. X. Fan, J. Jiang, Y. L. Wang, H. Zhang, L. H. Xie, W. Huang and T. Yu, Carbon, 2014 76, 148.

20 S. L. Kuo, W. R. Liu, C. P. Kuo, N. L. Wu and H. C. Wu, J. Power Sources, 2013, 244, 552.

21 D. W. Wang, C. H. Sun, G. M. Zhou, F. Li, L. Wen, B. C. Donose, G. Q. Lu, H. M. Cheng and I. R. Gentle, J. Mater. Chem. A, 2013, 1, 3607.

22 L. Yan, R. Y. Li, Z. J. Li, J. K. Liu, Y. J. Fang, G. L. Wang and Z. G. Gu, Electrochimica acta, 2013, 95, 146.

23 W. S. Hummers and R. E. Offeman, J. Am. Chem. Soc., 1958, 80, 1339.

24 N. I. Kovtyukhova, P. J. Ollivier, B. R. Martin, T. E. Mallouk, S. A. Chizhik, E. V. Buzaneva and A. D. Gorchinskiy, Chem. Mater., 1999, 11, 771.

25 Z. W. Xie, P. He, L. C. Du, F. Q. Dong, K. Dai and T. H. Zhang, Electrochimica acta, 2013, 88, 390.

26 C. Hontoria-Lucas, A. J. Lpez-Peinado, J. de D. Lopez-Gonzlez, M. L. Rojas-Cervantes and R. M. Martn-Aranda, Carbon, 1995, 33, 1585.

27 M. M. Hantel, T. Kaspar, R. Nesper, A. Wokaun and R. Kotz, Chem.-Eur. J., 2012, 18, 9125.

28 M. Seredych, J. A. Rossin and T. J. Bandosz, Carbon, 2011, 49, 4392.

29 S. Moussa, G. Atkinson, M. SamyEl-Shall, A. Shehata, K. M. AbouZeid and M. B. Mohamed, J. Mater. Chem., 2011, 21, 9608.

30 T. Kuila, S. Bose, P. Khanra, A. K. Mishra, N. H. Kim and J. H. Lee, Carbon, 2012, 50, 914.

31 Z. J. Fan, W. Kai, J. Yan, T. Wei, L. J. Zhi, J. Feng, Y. M. Ren, L. P. Song and F. Wei, ACS Nano, 2011, 5, 191.

32 S. Stankovich, D. A. Dikin, R. D. Piner, K. A. Kohlhaas, A. Kleinhammes, Y. Jia, Y. Wu, S. T. Nguyen and R. S. Ruoff, Carbon, 2007, 45, 1558.

Table 1 Fitted parameters of equivalent circuit of Fig. 1b

Electrodes	R_s (Ω)	R_{ct} (Ω)
GO-105	2.1	58
GO-130	2.0	53
GO-160	2.0	50
GO-180	2.1	44
GO-210	2.1	46
GO-250	2.0	48

Table 2 Fitted parameters of the elements on XPS for GO treated with different temperature

Samples	C/O ratio	Fitting of C1s (relative atomic percentage %)				
		C=C/C-C	C-OH	C-O-C	C=O	O-C=O
GO-105	2.03	44.9	49.1	3.4	1.5	1.5
GO-130	2.15	48.2	43.8	3.8	1.9	2.3
GO-160	2.76	68.7	22.4	1.4	2.9	4.6
GO-180	3.44	72.0	17.8	0	4.4	5.80
GO210	4.06	75.7	14.4	0	5.1	4.8
GO-250	4.88	78.2	14.3	0	5.8	1.7

Table 3 Fitted parameters of the elements on XPS for GO and GO-COOH

Samples	C/O ratio	Fitting of C1s (relative atomic percentage %)				
		C=C/C-C	C-OH	C-O-C	C=O	O-C=O
GO	2.20	40.5	52.2	3.8	1.9	1.6
GO-COOH	2.10	40.5	52.1	0	2.1	5.3

Figure.1

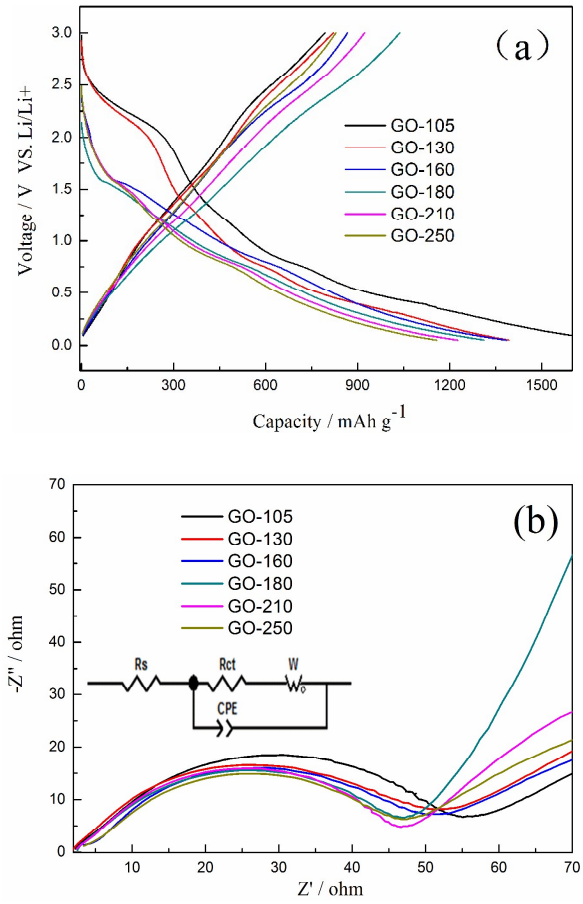

Fig. 1 The (a) charge and discharge curves and (b) AC impedance spectra with the equivalent circuit from the EIS measurements (inserted) of GO treated with different temperature.

Figure.2

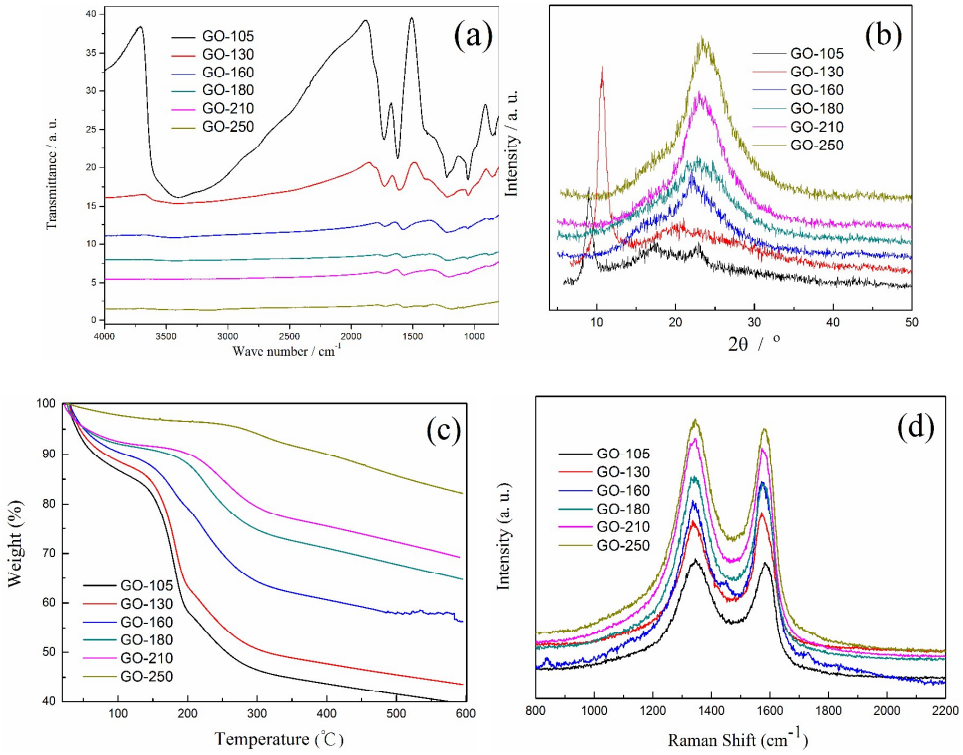

Fig. 2 (a) FT-IR, (b) XRD, (c) TGA and (d) Raman spectra of GO treated with different temperature.

Figure.3

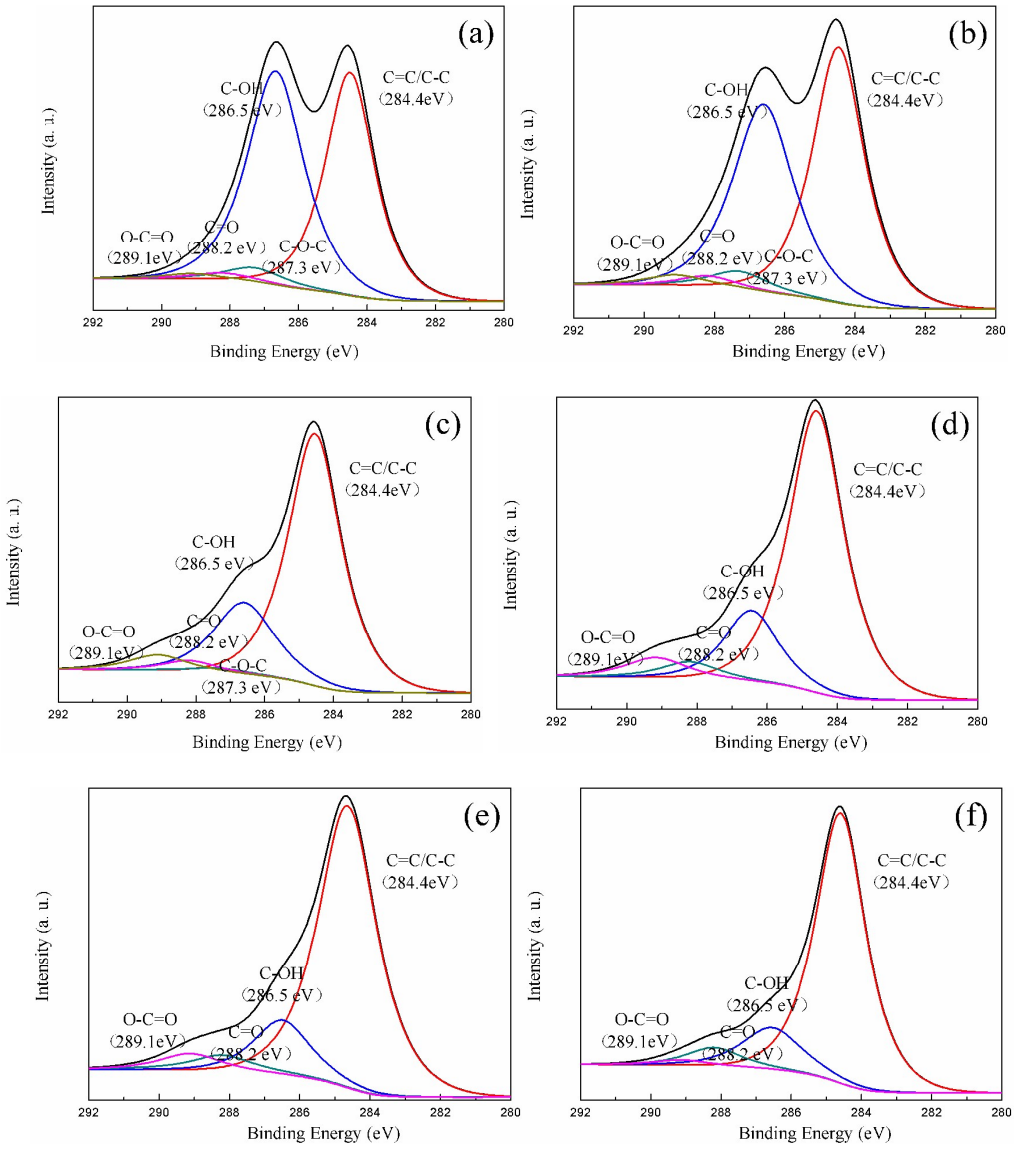

Fig. 3 Fitting results of C1s spectra of the GO treated with different temperature.

Figure.4

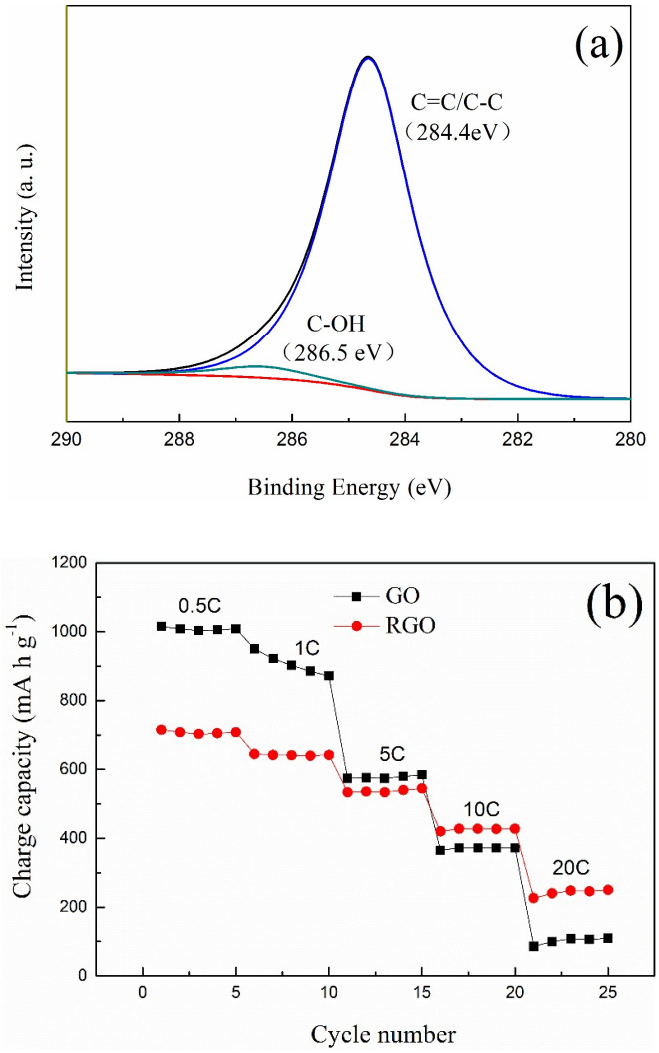

Fig. 4 (a) Fitting results of C1s spectra of the RGO and (b) the rate performance of GO and RGO electrodes.

Figure.5

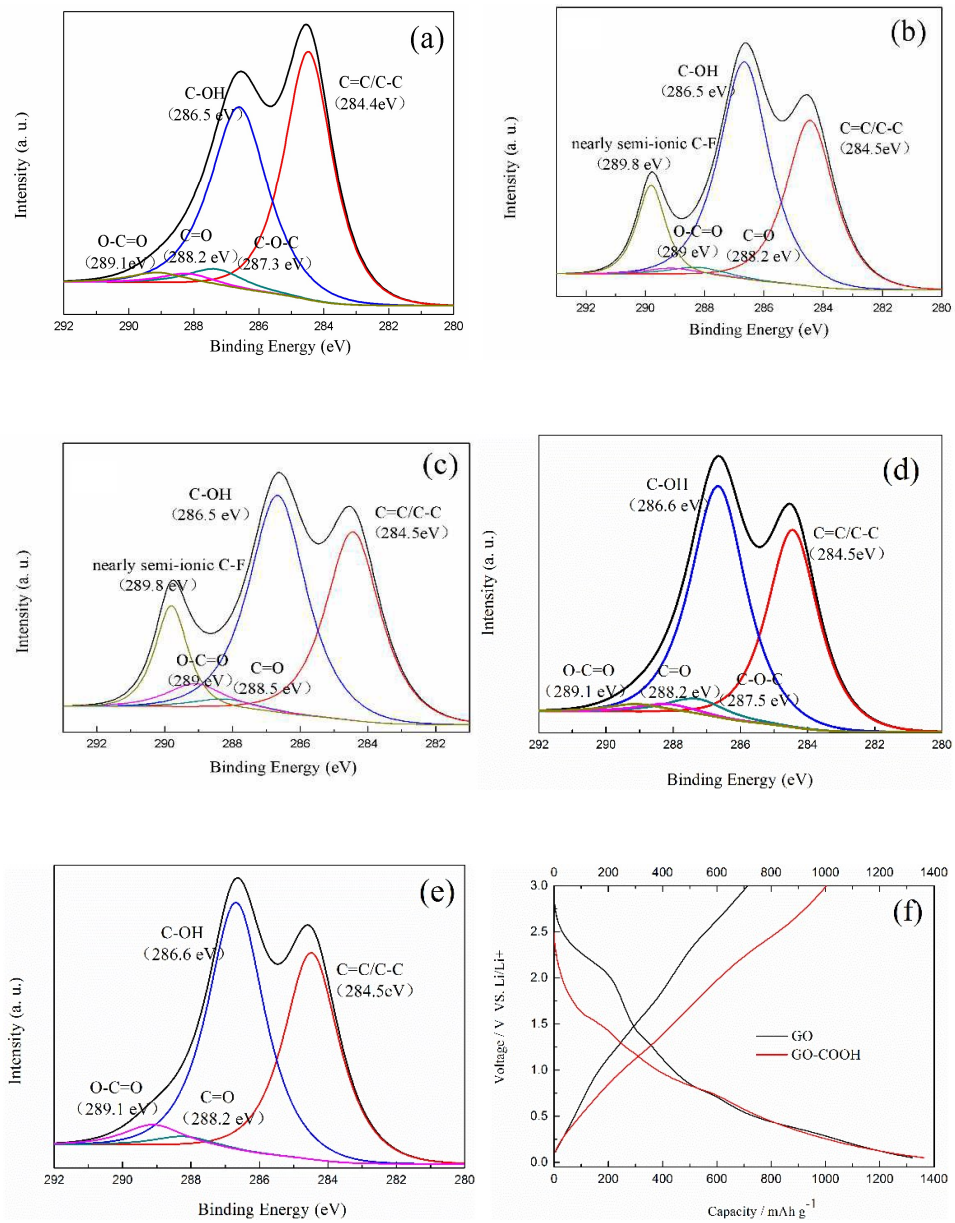

Fig. 5 Fitting results of C1s spectra of the GO-105 electrode (a) before charge and discharge cycle, (b) lithiated (c) delithiated state, (d)the initial GO and (e)GO-COOH; the (f) charge and discharge curves of GO and GO-COOH electrodes.